

Bomb-curve radiocarbon measurement of recent biologic tissues and applications to wildlife forensics and stable isotope (paleo)ecology

Kevin T. Uno^{a,1,2}, Jay Quade^b, Daniel C. Fisher^{c,d}, George Wittemyer^{e,f}, Iain Douglas-Hamilton^{f,9}, Samuel Andanje^h, Patrick Omondi^h, Moses Litoroh^h, and Thure E. Cerling^{a,i}

^aDepartment of Geology and Geophysics and ⁱDepartment of Biology, University of Utah, Salt Lake City, UT 84112; ^bDepartment of Geosciences, University of Arizona, Tucson, AZ 85721; ^cMuseum of Paleontology and ^dDepartment of Earth and Environmental Sciences, University of Michigan, Ann Arbor, MI 48109; ^eDepartment of Fish, Wildlife and Conservation Biology, Colorado State University, Fort Collins, CO 80523; ^fSave the Elephants, Nairobi 00200, Kenya; ⁹Department of Zoology, Oxford University, Oxford OX1 3PS, United Kingdom; and ^hKenya Wildlife Services, Nairobi 00100, Kenya

Edited by Mark H. Thiemens, University of California at San Diego, La Jolla, CA, and approved May 15, 2013 (received for review February 4, 2013)

Above-ground thermonuclear weapons testing from 1952 through 1962 nearly doubled the concentration of radiocarbon (¹⁴C) in the atmosphere. As a result, organic material formed during or after this period may be radiocarbon-dated using the abrupt rise and steady fall of the atmospheric ¹⁴C concentration known as the bomb-curve. We test the accuracy of accelerator mass spectrometry radiocarbon dating of 29 herbivore and plant tissues collected on known dates between 1905 and 2008 in East Africa. Herbivore samples include teeth, tusks, soft tissue, hair, and horn. Tissues formed after 1955 are dated to within 0.3–1.3 y of formation, depending on the tissue type, whereas tissues older than ca. 1955 have high age uncertainties (>17 y) due to the Suess effect. ¹⁴C dating of tissues has applications to stable isotope (paleo)ecology and wildlife forensics. We use data from 41 additional samples to determine growth rates of tusks, molars, and hair, which improve interpretations of serial stable isotope data for (paleo)ecological studies. ¹⁴C dating can also be used to calculate the time interval represented in periodic histological structures in dental tissues (i.e., perikymata), which in turn may be used as chronometers in fossil teeth. Bomb-curve ¹⁴C dating of confiscated animal tissues (e.g., ivory statues) can be used to determine whether trade of the item is legal, because many Convention of International Trade of Endangered Species restrictions are based on the age of the tissue, and thus can serve as a powerful forensic tool to combat illegal trade in animal parts.

carbon-14 | growth increments | growth rate | elephant | poaching

Carbon-14 (¹⁴C) is produced in the atmosphere primarily by neutron interaction with ¹⁴N through the reaction $^{14}\text{N} + n \rightarrow ^{14}\text{C} + p$. This occurs naturally from secondary neutron flux generated by cosmic rays and anthropogenically by high neutron flux from nuclear fission in bombs or, to a lesser degree, nuclear reactors. Atmospheric ¹⁴C is oxidized to CO₂, which enters the terrestrial biosphere through assimilation into plant biomass. Other living organisms incorporate ¹⁴C into their tissues by consuming plants or organisms that consume plants. ¹⁴C enters the oceans as CO₂ through air–sea exchange and subsequent vertical mixing and becomes part of the biologically available dissolved inorganic carbon pool. Following the inception of thermonuclear weapons testing, periodic measurement of atmospheric ¹⁴C concentrations began at stations around the world. These data document the abrupt rise and steady fall of ¹⁴C concentration in the atmosphere known as the bomb-curve. The atmospheric ¹⁴C concentration and its regional variation have been well known for the last 60 y (1, 2).

Previous studies testing bomb-curve ¹⁴C dating are largely limited to tree rings (1, 3) and a small number of mammal tissues (4, 5). Geyh (5) found human bone collagen and animal leather are less suitable for bomb-curve dating than hair, which could be used to determine age of death within about 2 y. Forensics research to determine year of birth has focused primarily on human tooth enamel and dentin (6–10), although proteins in the crystalline

portions of eye lenses also provide accurate birth-year estimates (11). Several studies have explored the use of radiocarbon to date tusk ivory (4, 12, 13) but offer only limited data and, in some cases, lower precision than accelerator mass spectrometry (AMS) methods (13).

Here we use animal and plant tissues of known ages to expand significantly on previous studies in the number of samples and tissue types to show that from 1955 to the present ¹⁴C-calibrated ages measured by AMS accurately record the date during which the tissues formed. We demonstrate the accuracy of bomb-curve ¹⁴C dating based on results from 29 apatite, collagen, keratin, soft tissue, and plant samples. Maximum accuracy with respect to the known age is achieved by using tissues that undergo little or no turnover. Samples collected from the proximal, or most recently formed, portion of the tissue can be used to determine date of collection, which is often, but not always, death.

Using an additional 41 ¹⁴C ages, we determine tissue growth rates by serially sampling along the growth axes of *Hippopotamus amphibius* (hippo) canines and *Loxodonta africana* (elephant) tusks, molars, and tail hair. We provide examples of how ¹⁴C ages from these mammal tissues can be used in stable isotope (paleo)ecology and wildlife forensics. In stable isotope ecology, growth rates are required to convert distance along the growth axis of a tissue to time, which enables comparison of isotope data with time-series data (e.g., temperature, rainfall, or remote sensing data such as Normalized Difference Vegetation Index). ¹⁴C-derived growth rates from extant species can also be used to determine the period (e.g., days or weeks) represented in growth increments in dental tissues, providing a basis for establishing a chronometer in fossil teeth. Chronologic control is imperative in intratooth stable isotope and histological studies that aim to evaluate seasonal variability in past environments. Finally, we demonstrate that ¹⁴C dating can be used in wildlife forensics to determine the age of confiscated animal tissues, which in many cases is equivalent to the date of death. For many animal parts, such as ivory and rhino horn, age often determines whether trade of the item is legally permitted.

Results

Fraction Modern Carbon and ¹⁴C-Calibrated Ages. ¹⁴C data are presented as fraction modern carbon (F¹⁴C), where $F^{14}\text{C} = (A_s / 0.95 A_{\text{Ox}}) \times (0.975/0.981)^2 \times [(1 + \delta^{13}\text{C}_{\text{Ox}}/1,000)/(1 + \delta^{13}\text{C}_s/1,000)]$

Author contributions: K.T.U., G.W., and T.E.C. designed research; K.T.U., J.Q., D.C.F., G.W., I.D.-H., S.A., P.O., M.L., and T.E.C. performed research; D.C.F. contributed new reagents/analytic tools; K.T.U., J.Q., D.C.F., and T.E.C. analyzed data; and K.T.U. wrote the paper.

The authors declare no conflict of interest.

This article is a PNAS Direct Submission.

¹Present address: Division of Biology and Paleo Environment, Lamont-Doherty Earth Observatory of Columbia University, Palisades, NY 10964.

²To whom correspondence should be addressed. E-mail: kevinuno@ldeo.columbia.edu.

This article contains supporting information online at www.pnas.org/lookup/suppl/doi:10.1073/pnas.1302226110/-DCSupplemental.

1,000)]²; A is the activity or ¹⁴C/¹²C ratio, δ¹³C is the carbon isotope ratio, and the subscripts S and OX are for the sample and the oxalic acid standard, respectively (14). Where appropriate, we also use the Δ¹⁴C notation, expressed in permil notation (‰), where Δ¹⁴C = [(F¹⁴C) e^{λ(1950-y)} - 1] × 1,000, where λ is 1/8,267 and year is the year the sample was analyzed. Calibrated ¹⁴C ages were determined with the software program CALIBomb (15) (SI Text).

The F¹⁴C values plotted against the known age reveal that the F¹⁴C in herbivore and plant samples tracks the F¹⁴C of atmospheric CO₂ during the period in which the tissue formed for samples collected after 1955 (Fig. 1A). Pertinent sample information is provided in Dataset S1, Table S1, and all F¹⁴C-, Δ¹⁴C-, and ¹⁴C-calibrated ages are given in Dataset S1, Table S2. The Northern Hemisphere 3 (NH3) and Southern Hemisphere 1 (SH1) calibration curves (1) are both plotted in Fig. 1A because we sampled animal tissues from both regions. The NH3 data set is appended with the Levin dataset (2, 16) (NH3+Levin) beginning at 1999.50 to permit ¹⁴C age calibration through 2006. The two curves, NH3+Levin and SH1, differ significantly before ~1970 owing to bomb testing locations and atmospheric circulation, and subtle differences of 4–5‰ persist after 1970. Pre-1970 keratin and plant samples are confirmed (or in several cases presumed) to have been collected from the Southern Hemisphere and track the SH1 curve extremely well (Fig. 1A).

Fig. 1B shows the known age versus the calibrated ¹⁴C age for all samples (n = 22) collected from 1955 to 2006. Fig. 1C includes four samples collected between 1905 and 1953 to illustrate the inaccuracy of calibrated ¹⁴C ages before 1955. The residual (r) between the ¹⁴C age (age_{14C}) and known age (age_{known}) is given by r = age_{14C} - age_{known} (Fig. S1 and Dataset S1, Table S2). The mean residual of 11 keratin samples collected after 1955 is -1.3 ± 1.8 (1σ) years. For apatite samples (n = 5), the mean residual is -0.8 ± 0.7 y; for grasses (n = 3), it is 0.3 ± 0.6 y. For the soft tissue and collagen samples, the residuals are -0.7 and -1.2 y, respectively. Variation in mean residuals based on tissue type likely arises from differences in the total number of samples analyzed, in the amount of time integrated in different tissue types, and in the F¹⁴C values (e.g., whether the samples fall on a steep or shallow part of the bomb-curve). Tissues formed during the steeper parts of the bomb-curve tend to have residuals less than 2 y (Fig. S1). The current slope of the bomb-curve is shallower than during the interval from 1955 to ca. 2005, increasing the uncertainty of ¹⁴C-calibrated ages in tissues formed from ca. 2005 forward (Fig. 1A and Dataset S1, Table S2).

A hair sample (L10830) from a *Cercopithecus mitis* (blue monkey) was reportedly collected in the Congo in 1962 but has a F¹⁴C value of 0.9749 ± 0.0023 (this and all subsequent SDs are 2σ), which clearly indicates it formed before 1955. Nearly

70% of the blue monkey's diet is fruit and leaves, so significant dietary contribution from older plant material (more than several years old) is unlikely (17). Hair from other primates, including two other *C. mitis*, yield ¹⁴C ages consistent with known dates, further suggesting that diet is not the cause for the age discrepancy. The most likely explanation is that the date of museum accession, which we used as the known age of the sample, does not reflect the date of death.

Tissue Growth Rates. We use multiple ¹⁴C ages from elephant tusks, molar plates, and tail hair and hippo canines to calculate tissue growth rates (Table 1). A schematic of the general structure of tusks, molars, and canines is shown in Fig. S2. The period of growth for some canines and both tusks continued beyond 1997, when ¹⁴C data becomes sparse for both the NH3 and the SH1 data sets. Thus, we use the Levin dataset to calibrate ¹⁴C ages for samples more recent than 1960 with an F¹⁴C ≤ 1.110.

Elephant tusks. Tusk growth rates for two female African elephants were determined from collagen-derived ¹⁴C ages. Growth rates are 4.13 ± 0.39 cm/y and 5.10 ± 0.74 cm/y for elephants R37 and Misha, respectively (Fig. 2A and Table 1). We use linear growth rates because they best fit the data from the two tusks, although a second-order polynomial also fits the tusk data from R37. Because there is no calibrated ¹⁴C age for the youngest data point for Misha, we use September 10, 2008, her known date of death.

Assuming an age at death of 53 ± 5 y for R37 based on molar wear (18, 19), the R37 tusk represents growth from 25 to 53 y of age, whereas Misha's tusk represents growth from 13 to 28 y of age. Thus, the 20% difference in growth rate between the two tusks may be explained by ontogeny, but may also relate to captive (Misha) versus wild (R37) diet or stress levels. Although linear growth rates are appropriate for the two tusks, our data suggest for tusks that record multiple ontogenetic stages (e.g., juvenile, adolescent, and adult), growth rates may not be linear. Mastodon tusks show nonlinear growth rates based on measurements of annual incremental thicknesses and lengths over ~30 y (20, 21). Using the tusk lengths and growth rates for R37 and Misha, we calculate the time represented in the tusks to be 28.0 and 14.8 y, respectively (Table 1). Interestingly, this accounts for 54% and 53% of their total lifespans, respectively, suggesting similar overall rates of wear between the two female elephants. Additional ¹⁴C ages from tusks that formed between 1955 and 2005, particularly from male tusks and tusks that capture multiple ontogenetic stages, would elucidate variation in tusk growth rate as a function of sex and age.

Hippo canines. We calculate growth rates for five hippo canines using a total of 17 enamel ¹⁴C ages. Length measurements are made along the outer curve of the canine. Multiple ¹⁴C ages from a lower (n = 5) and an upper (n = 3) canine of an individual, presumed to be a juvenile or young adult based on canine shape

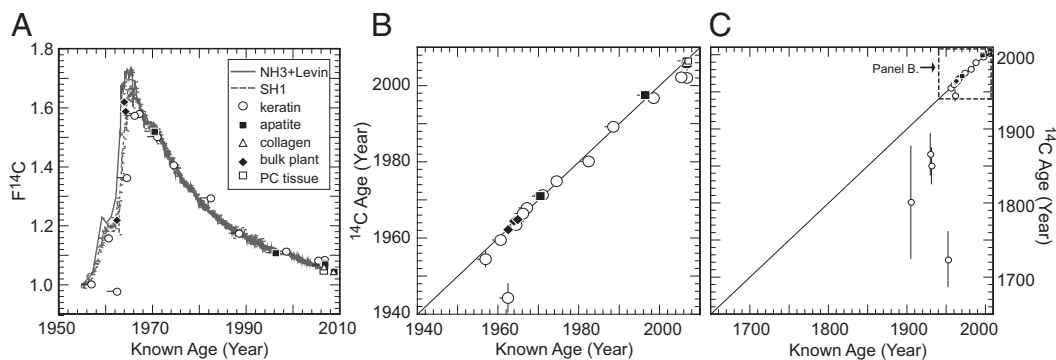


Fig. 1. (A) Fraction modern carbon (F¹⁴C) vs. known age (year), where known age is determined by the known date of death or collection for post-1955 tissue and plant samples. The y-axis uncertainty is smaller than the symbols. Calibrated ¹⁴C age vs. known age for tissues and plants for (B) samples younger than 1955 (n = 23) and (C) all samples (n = 27). The y-axis uncertainty is 2σ; one-way x-axis uncertainty on some samples in A and B represents potential offset of up to 2 y between the actual date of death and date of collection or accession.

Table 1. Tissue growth rates determined from calibrated ¹⁴C ages

| Sample ID | Growth rate ± 2σ | Length, cm | Proximal ¹⁴ C age | Distal ¹⁴ C age | Time in tissue, y |
|---|------------------|------------|------------------------------|----------------------------|-------------------|
| Tail hair (keratin), mm/d | | | | | |
| TSV-171 | 0.81 ± 0.77 | 31.4 | 1996.7 | 1996.0 | 0.7 |
| R37 | NA | | 2001.9 | 2002.5 | — |
| Hippo canines (bioapatite), cm/y | | | | | |
| 2KL (upper) | 1.94 ± 0.31 | 17.0 | 1969.5 | 1964.2 | 8.8 |
| KL | 3.35 ± 0.25 | 37.2 | 1960.0 | 1970.6 | 11.1 |
| K11-KF | 4.51 ± 0.41 | 35.0 | 1979.0 | 1972.4 | 7.8 |
| K08-201 | 4.87 ± 0.34 | 56.0 | 2006.5 | 1996.8 | 11.5 |
| TSV-291 | 7.47 ± 0.88 | 60.0 | 1996.9 | 1989.6 | 8.0 |
| Elephant tusks (collagen), cm/y | | | | | |
| Misha | 5.11 ± 0.75 | 73.0 | 2008.7 | 1993.9 | 14.8 |
| R37 | 4.13 ± 0.39 | 115.6 | 2005.5 | 1978.1 | 28.0 |
| Elephant molar plates (bioapatite), cm/y | | | | | |
| TE-95 Rm6.2 | 1.49 ± 0.54 | 10.1 | 1959.3 | 1955.0 | 6.8 |
| TE-95 Rm6.4 | 1.46 ± 0.59 | 11.6 | 1959.7 | 1954.3 | 7.9 |
| TE-95 Rm6.7 | 1.63 ± 0.14 | 12.3 | 1963.1 | 1957.1 | 7.5 |
| TE-95 Rm6.9 | 1.62 ± 0.14 | 11.1 | 1963.9 | 1959.1 | 6.9 |
| R37 Lm6.7 | 1.39 ± 0.27 | 7.8 | 1984.2 | 1979.6 | 5.6 |
| R37 Lm6.10 | 1.61 ± 1.19 | 5.9 | 1988.4 | 1986.3 | 3.7 |

Total time represented in tissue is based on growth rate and length.

and size, give linear growth rates of 3.35 ± 0.25 cm/y and 1.94 ± 0.31 cm/y, respectively (Fig. 2B). Growth rates from three other (lower) canines, presumably from males based on size, range from 4.51 ± 0.21 cm/y to 7.47 ± 0.88 cm/y (Table 1 and Fig. 2C). Passey et al. (22) measured lower canine growth rates in two female hippos from the Toledo Zoo by notching the tooth at the gum line and measuring the distance from the gum line the following year. Growth rates from the 48- and 8-y-old females were 1.35 cm/y and 2.9 cm/y, respectively. These are lower than the values determined for lower canines in this study (3.35–7.47 cm/y), which is likely due to differences in canine growth rates between male and female hippos and, for the 48-y-old individual, age.

Elephant molars. We calculate vertical growth rates along six plates from two molars using a total of 16 ¹⁴C ages. These growth rates are time-averaged mineralization rates of enamel, which may differ from molar extension rate. The latter is determined by the extension of the molar plate as new dentin and immature enamel are formed, whereas the former represents the difference between the average ages of the enamel volumes sampled at each position along the plate. If molar extension and enamel maturation processes were constant throughout molar formation, then mineralization and extension rates would be equal. Fig. 3A shows sample locations in the third molar (m3) from

TE-95. Growth rates were determined in four plates (2, 4, 7, and 9) in sample TE-95 and two plates (7 and 9) in R37's m3. Growth rates from both molars range from 1.39 ± 0.27 to 1.63 ± 0.14 cm/y (Table 1 and Fig. 3B and C). The rates fall within the range of those determined histologically for the extinct Columbian mammoth (*Mammuthus columbi*): 1.3–2.2 cm/y (23, 24). The ¹⁴C data do not reveal whether growth rates are linear; however, histological data from two extinct proboscidean species, *M. columbi* and *Paleoloxodon cypristes*, indicate growth rates are highest near the initial occlusal surface and decrease toward the cervical margin (23).

A ¹⁴C age on collagen from the mesial root of TE-95 yields an age of 1964.2 ± 0.1 , which is the best estimate for the date of death (Fig. 3A). Time represented in unworn molar plates from TE-95 is 7.3 ± 0.6 y, and time represented in an entire elephant molar is ca 0.10 y or more based on ¹⁴C ages from TE-95 and R37 (Table 1). The thick enamel and the long time intervals represented in a single plate or entire molar make fossil proboscidean teeth excellent candidates for intratooth stable isotope profiles in paleoecology (e.g., ref. 25).

Elephant tail hair. Only one of two tail hairs sampled provides a reasonable growth rate. Sample TSV-171, collected on July 17, 1998, from a female African elephant in Tsavo National Park,

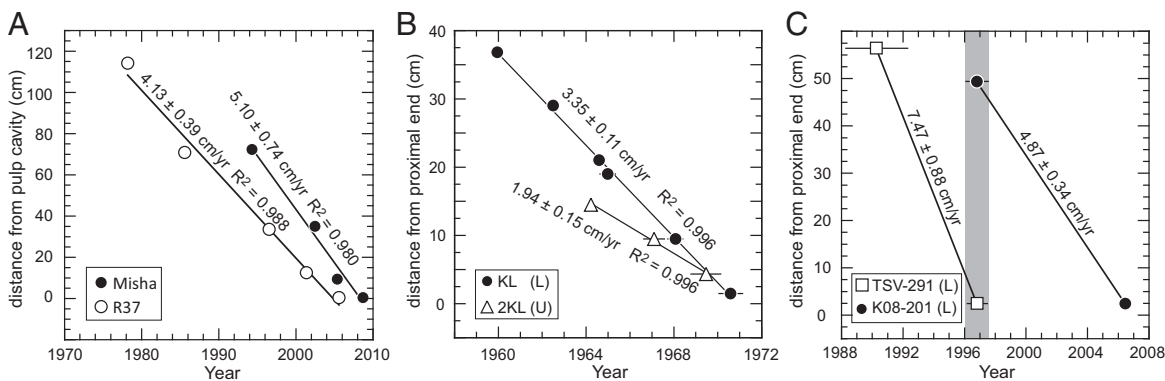
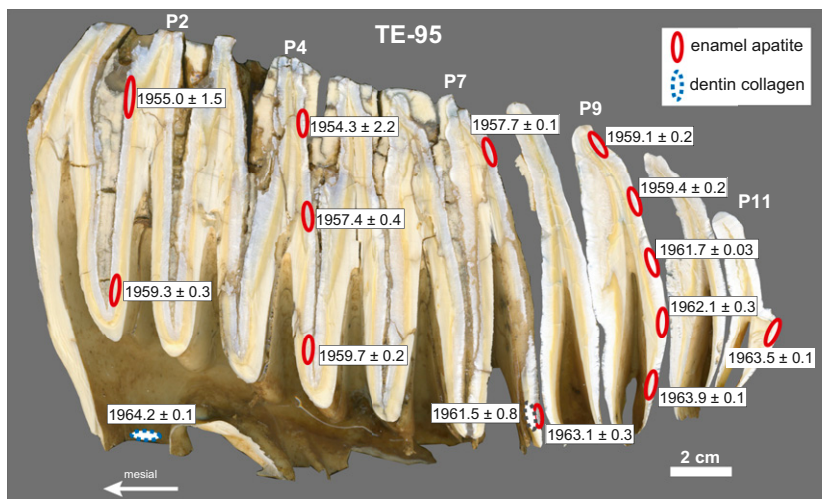
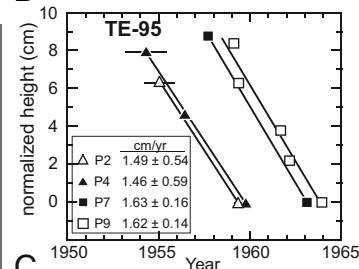


Fig. 2. Calculated linear growth rates for (A) two tusks of female African elephants, (B) upper (U) and lower (L) hippo canines collected from an individual in Queen Elizabeth National Park, Uganda in 1971, and (C) lower canines from two hippos from Tsavo National Park, Kenya whose lives overlapped by ca. 1 y (shaded area). Growth rates ($\pm 2\sigma$) are calculated from the slope of the regression lines. Calibrated ¹⁴C age uncertainty is 2σ and if not shown is smaller than the symbol.

A



B



C

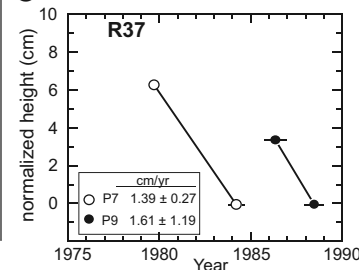


Fig. 3. (A) Longitudinally cut elephant molar (m3) from individual TE-95 showing calibrated ^{14}C ages ($\pm 2\sigma$) for 13 enamel apatite and 2 dentin collagen samples. Sample locations are outlined as ellipses. The molar consists of 11 enamel-covered plates (P1 to P11). (B) Vertical growth rates from four TE-95 molar plates shown in A are calculated from ^{14}C ages. (C) Vertical growth rates in two molar plates from a lower third molar belonging to R37 (see text). Growth rates ($\pm 2\sigma$) are calculated from slopes; height along a plate is normalized to the lowest sample location. Age uncertainty is 2σ and if not shown is smaller than the symbol.

yields a growth rate of 0.81 ± 0.77 mm/d (Table 1). Wittemyer et al. (26) used independent methods to calculate a growth rate of 0.81 ± 0.11 mm/d for female African elephants ($n = 38$). A second tail hair was collected from R37 within days of her death in September 2006. The proximal and distal ends of the 304-mm-long hair have nearly identical $F^{14}\text{C}$ values of 1.0820 and 1.0803, respectively, and the higher value in the proximal end precludes calculating a growth rate. Growth rates determined by independent methods from R37 tail hairs collected between 2001 and 2006 range from 0.56 to 0.62 mm/d.

^{14}C variation based on tissue type and pretreatment. Four tissue types were sampled at death from two elephants to test for variation in ^{14}C based on tissue type. Collagen and apatite from tusk dentin sampled from the pulp cavity margin (e.g., the tissue forming at time of death) show indistinguishable $F^{14}\text{C}$ values (Dataset S1, Table S3). The $F^{14}\text{C}$ values can be used to calculate a ^{14}C -calibrated age for R37, and the collagen and apatite ages fall within a range of less than 0.4 y. We tested whether treating tusk apatite with 3% NaOCl had any effect on $\Delta^{14}\text{C}$ values. Treated and untreated apatite samples from Misha have nearly identical $\Delta^{14}\text{C}$ values, whereas those from R37 differ by 5.6‰ but fall within the range of 2σ uncertainty (Dataset S1, Table S3). The data suggest treatment to oxidize organics before acid digestion is not necessary.

We also analyzed the proximal end of a tail hair (R37-prox-K) and soft tissue from R37's tusk pulp cavity (R37-PC-tissue). The $F^{14}\text{C}$ value in the tail hair is anomalously high, resulting in an older age than the actual date of death (Dataset S1, Table S3). The soft tissue sample has a $\Delta^{14}\text{C}$ value of 43.7‰ and a ^{14}C -calibrated date of 2006.04, which is the closest to the actual date of death of all R37 tissues analyzed.

Discussion

Application to Stable Isotope (Paleo)ecology. ^{14}C -correlated stable isotope profiles. Serial sampling or intratooth stable isotope profiles of enamel yield information about seasonal change in diet and water use, which relate to seasonality of precipitation and vegetation. This has been suggested as a method for (paleo)dietary and (paleo)ecological reconstruction in modern and fossil mammalian teeth (e.g., refs. 25, 27–31). In ungulate molars, tooth height and growth rate determine total formation time, which is

generally no more than 2–3 y (32, 33). However, continuously growing teeth from large mammals (e.g., hippo canines and elephant tusks) and elephant molars form over years to decades and therefore can be used to evaluate long-term dietary and seasonality changes (28, 31, 34) and can capture ontogenetic transitions such as weaning (35).

We show that intratooth stable isotope profiles from two hippos that died nearly 11 y apart can be concatenated (with sufficient overlap) using ^{14}C data (Fig. 4). ^{14}C data come from two canines, one collected in 1996 (TSV-291) and the other in 2008 (K08-201), from the same region near Tsavo National Park. The $F^{14}\text{C}$ values from enamel in the proximal end of the 1996 and the distal end of the 2008 canines are nearly identical and therefore yield similar ^{14}C ages (Fig. 4). The dominant feature in the $\delta^{13}\text{C}$ record from the TSV-291 canine is a rapid decrease of 5.4‰,

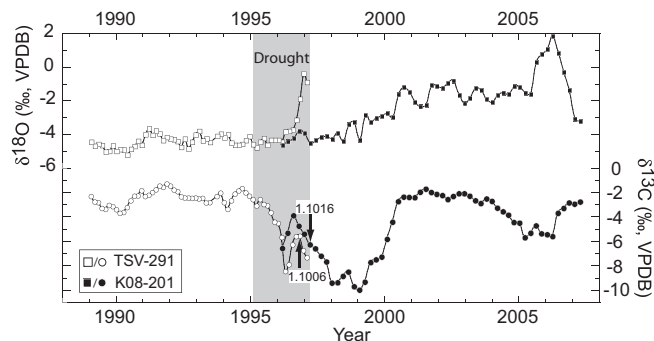


Fig. 4. Intratooth stable isotope profiles from two hippo canines overlap to provide a continuous 18-y isotope record. $F^{14}\text{C}$ values used as a tie point between the two canines are labeled with arrows indicating sample location. Based on the shape of the $\delta^{13}\text{C}$ curves, the K08-201 profile has been shifted $\sim +0.3$ y, which is within the 2σ range of uncertainty. Canine TSV-291 was collected in 1996 near the town of Mtito Andei, Kenya. The steep rise in $\delta^{18}\text{O}$ that begins ~ 200 d before death suggests physiological stress preceding death, a pattern observed in other serially sampled hippo canines. Canine K08-201 is from a hippo shot dead on October 10, 2007 as a (crop-raiding) nuisance animal near Mtito Andei.

indicating a switch to (C_3) browsing beginning in the latter part of 1995, followed by a 4‰ increase in $\delta^{18}O$ during last half year of the hippo's life in 1996 (Fig. 4). The onset of the $\delta^{13}C$ shift coincides with beginning of a prolonged drought that persisted until April of 1997. The 2008 canine suggests that browsing diets persisted among hippos in this region until the year 2000, when the diet returns to predominantly C_4 grazing.

Overlapping isotope profiles from multiple teeth based on bomb-curve ^{14}C ages can provide long-term ecological records. These records may be useful for tracking decadal (or longer) scale changes in land-use, climate, or life-history patterns and thus have potential application in wildlife ecology and conservation. Understanding how ecological change, such as periods of drought or seasonal precipitation, affects intratooth isotope profiles in extant taxa provides insight for interpreting profiles in fossil teeth.

Periodicity of incremental growth features. Periodic incremental growth features in tooth enamel and dentin (e.g., perikymata, striae of Retzius, and Andresen lines) can be used as accurate chronometers if the time interval represented by each increment is known (36). By establishing a chronometer, the teeth can provide information about the timing of tooth development and other aspects of life history. The chronometer is critical for interpreting intratooth stable isotope profiles in fossil teeth, where one of the primary goals is to determine the magnitude, duration, and periodicity of dietary or environmental change in the past. In most human and some other hominin teeth, perikymata visible on the surface of a tooth represent a period of 7 or 8 d (37). In proboscidean tusks, three hierarchical incremental growth features have been proposed: First-order increments have annual periodicity, second-order are weekly in elephants and mammoths (fortnightly in mastodons), and third-order are daily (38, 39).

We use ^{14}C growth rates to determine the time interval represented in hippo canine perikymata and to confirm the weekly time interval represented in elephant tusk dentin. The distance between perikymata was measured along sections of canine K11-KF using a plugin (Inc Meas v.1.2) in ImageJ software (Fig. S3). Mean increment width is 1.26 ± 0.35 mm ($n = 167$), and given the growth rate of 45.1 mm/y, each increment represents 10.2 ± 2.9 (1σ) days (Dataset S1, Table S3). Other hippo canines for which ^{14}C growth rates were determined either lacked visible perikymata or photos for making measurements.

In the R37 tusk, we measured the thickness of second-order increments on a transversely cut thin section located 2 mm from the horn of the pulp cavity using the same ImageJ plugin (Fig. S4). The average growth rate determined from histological measurements is 103 ± 29 $\mu\text{m}/\text{wk}$ (Dataset S1, Table S4), whereas the ^{14}C growth rate is 105 ± 11 $\mu\text{m}/\text{wk}$ (Dataset S1, Tables S5 and S6). The ^{14}C growth rate provides independent evidence for weekly periodicity of second-order growth increments in elephant tusk dentin.

The period recorded in growth increments in modern teeth and tusks can be applied with caution, because the period between increments may differ between modern and fossil teeth, to similar taxa in the fossil record that cannot be bomb-curve radiocarbon-dated, and thus provide a chronometer in fossil teeth. This is particularly useful for intratooth stable isotope profiles or histological data that are used to evaluate seasonality (e.g., ref. 31).

Application of ^{14}C Dating to Wildlife Forensics. The international trade in animal parts, defined here as sale, purchase, import, export, or re-export, is a booming industry estimated to value \$5–15 billion annually (40). Although corresponding numbers for the illegal trade are not known, the United Nations Environment Program estimated its value in 1998 to be on the order of \$5–8 billion per year, whereas other sources argue the current value is twice this amount (41).

The Convention of International Trade of Endangered Species (CITES) treaty, national, and regional (e.g., European Union) regulations ban the trade of modern ivory. However, there are many exceptions in which trade is legal, and nearly all depend on the age of the ivory (details in SI Text). For example,

in the United States interstate trade is legal for raw or worked African elephant ivory if it was imported before 1989. The demand for ivory, and hence poaching, has risen dramatically since 2006 despite the CITES ban on trade of modern ivory (42–44).

Given the dependence of trade status on the age of ivory, ^{14}C dating of ivory serves as a forensics tool to assess whether trade is legal. Our results show that ivory apatite and collagen are both suitable for ^{14}C dating (Dataset S1, Table S3), but because collagen requires less powdered ivory (~25–50 mg) than apatite (150 mg) for analysis, collagen is preferable when sample availability is limited, as is often the case with small figurines or jewelry. Because there are at least two possible ages for each $F^{14}C$ value, if the question of the age of ivory is not simply whether the animal part is pre- or postbomb, then at least two samples must be taken from the specimen and the orientation of the growth axis must be known to ascertain the correct age (SI Text).

Other forensic tools have been developed for geolocating the origin of ivory, such as DNA (45), stable isotope analysis ($\delta^{13}C$, $\delta^{15}N$, and $^{87}Sr/^{86}Sr$) (46, 47), and measurements of Schreger bands to differentiate between Asian and African elephant ivory (48). For confiscated ivory with an unknown origin, combined geolocating and ^{14}C dating methods can determine the source and age of ivory and, as a result, whether trade is legal. This information can help identify where and when areas are being exploited for illegal trade, which is critical for directing conservation and antipoaching resources. The ^{14}C dating method can be extended to other animal parts such as hair and horn (e.g., from rhinos), as indicated by our results on keratin samples of known age (Fig. 1 and Dataset S1, Table S2).

Conclusions

In this study, we show bomb-curve ^{14}C can be used to accurately date keratin, collagen, apatite, and bulk plant tissue, and we provide examples of applications of the technique to stable isotope (paleo)ecology and wildlife forensics. Plant and animal tissues that formed between 1955 and 2008 have been accurately dated (-0.9 ± 1.4 y, 1σ) for 21 samples of known age using bomb-curve ^{14}C . Our results from all post-1955 tissues indicate their carbon was derived from recently photosynthesized CO_2 (within ca. 1 y of sampling), regardless of tissue type and across a range of biological isotope enrichment factors.

We calculated growth rates of elephant tail hair, tusks, molars, and hippo canines from multiple ^{14}C ages measured along tissue growth axes. ^{14}C measurements from NaOCl-treated dentin, untreated dentin, and collagen from two elephant tusks yield indistinguishable ages, indicating both apatite and collagen are suitable for bomb-curve ^{14}C dating, and that treatment of dentin apatite to remove organics is not necessary for ^{14}C measurement.

Our results have the following immediate and unique applications to stable isotope (paleo)ecology and wildlife forensics. We concatenated intratooth $\delta^{13}C$ and $\delta^{18}O$ profiles from two hippo tusks using ^{14}C ages to establish a tie point, resulting in an 18-y composite stable isotope record. Records such as these can be used to study long-term (i.e., multidecadal) population, climate, or ecosystem dynamics that would not be feasible from a single intratooth profile, exclusive of proboscidean tusks. Growth rates from bomb-curve ^{14}C dating can be used to determine the time represented in periodic growth increments. Determining the time represented in periodic growth increments in teeth of extant taxa provides a potential chronometer in fossil teeth, where knowledge of growth rate is critical to interpretation of intratooth stable isotope profiles or histological data related to life history.

^{14}C dating of raw or worked animal tissues can be used to establish sample age and in many cases date of death of an animal, which can determine whether trade is legal according to CITES or other regulations. Poaching for elephant tusks and rhino horn has increased significantly since 2006. Turnaround time and cost of AMS ^{14}C measurements have decreased in the past decades, and therefore it is an accessible wildlife forensics tool. Combined with geolocation (e.g., DNA, stable isotope, and

histological) forensic techniques, ^{14}C dating of animal parts can help budget-limited government agencies and nongovernmental organizations determine how and where to direct conservation and anti-poaching resources.

Materials and Methods

Sampling and analytical procedures are described in detail in *SI Text*. Briefly, inorganic tissues (bioapatite from dentin and enamel) were digested offline in 104% (by density) phosphoric acid to generate CO_2 . Organic tissues (keratin, collagen, and bulk plant tissue) were combusted in sealed quartz tubes at 850°C for 4 h in the presence of CuO and Ag foil to generate CO_2 . CO_2 was cryogenically purified, graphitized, and measured for ^{14}C by AMS at the University of Arizona. Stable carbon isotope ratios are reported as δ values relative to the Vienna Pee Dee Belemnite (VPDB) standard using permil (‰) notation, where $\delta^{13}\text{C} = (R_{\text{sample}}/R_{\text{standard}} - 1) \times 1,000$, and R_{sample}

and R_{standard} are the $^{13}\text{C}/^{12}\text{C}$ ratios in the sample and in the standard, respectively. The $\delta^{13}\text{C}$ values are used for fractionation corrections of ^{14}C .

ACKNOWLEDGMENTS. We thank the Office of the President of the Republic of Kenya, the Kenya Wildlife Service (KWS), and the Samburu and Buffalo Springs County Councils for permission to conduct this research. We thank the KWS, Save the Elephants, the National Museums of Kenya, the Field Museum of Natural History, Prince Kaleme (Centre de Recherche en Sciences Naturelles, Lwiro, Democratic Republic of the Congo), N. Carpenter (Utah's Hogle Zoo), H. Klingel, and F. Kirera for sample collection or providing access to collections. K.T.U. thanks A. Rountrey for furnishing a copy of the plug-in (Inc Meas v. 1.2) used to measure growth increments in ImageJ. We thank K. Chrzt, A. Copeland, B. Hethmon, and J. Singer for assistance with sample preparation. We thank two anonymous reviewers for comments. This research was supported by National Science Foundation Grants EAR-0819611 and BCS-0621542 (to T.E.C.), the National Geographic Society (T.E.C.), and by a University of Utah Graduate Research Fellowship (to K.T.U.). This work was carried out under CITES permits US831854/9, 02US053837/9, and 07US159997/9.

- Hua Q, Barbetti M (2004) Review of tropospheric bomb ^{14}C data for carbon cycle modeling and age calibration purposes. *Radiocarbon* 46(3):1273–1298.
- Levin I, Kromer B (2004) The tropospheric $^{14}\text{CO}_2$ level in mid-latitudes of the Northern Hemisphere (1959–2003). *Radiocarbon* 46(3):1261–1272.
- Hua Q, Barbetti M, Worbes M, Head J, Levchenko VA (1999) Review of radiocarbon data from atmospheric and tree-ring samples for the period 1945–1997 AD. *IAWA J* (20):261–284.
- Vogel J, Fuls A, Visser E (2002) Accurate dating with radiocarbon from the atom bomb tests. *S Afr J Sci* 98:437–438.
- Geyh MA (2001) Bomb radiocarbon dating of animal tissues and hair. *Radiocarbon* 43:723–730.
- Spalding KL, Buchholz BA, Bergman LE, Druid H, Frisén J (2005) Forensics: Age written in teeth by nuclear tests. *Nature* 437(7057):333–334.
- Cook GT, Dunbar E, Black SM, Sheng X (2006) A preliminary assessment of age at death determination using the nuclear weapons testing ^{14}C activity of dentine and enamel. *Radiocarbon* 48(3):305–313.
- Ubelaker DH, Buchholz BA, Stewart JEB (2006) Analysis of artificial radiocarbon in different skeletal and dental tissue types to evaluate date of death. *J Forensic Sci* 51(3):484–488.
- Wang N, et al. (2010) Improved application of bomb carbon in teeth for forensic investigation. *Radiocarbon* 52(2):706–716.
- Buchholz BA, Spalding KL (2010) Year of birth determination using radiocarbon dating of dental enamel. *Surf Interface Anal* 42(5):398–401.
- Lynnerup N, Kjeldsen S, Heegaard S, Jacobsen C, Heinemeier J (2008) Radiocarbon dating of the human eye lens crystallines reveal proteins without carbon turnover throughout life. *PLoS One* 3(1):e1529.
- Sideras-Haddad E, Brown T (2002) Dating studies of elephant tusks using accelerator mass spectrometry. *Proceedings of the Ninth International Conference on Accelerator Mass Spectrometry* (Elsevier, New York).
- Brunnermeier MJ, Schimidt SAK, Müller-Boge M, Schupfner R (2012) Dating of ivory from 20th century by determination of ^{14}C by the direct absorption method. *Appl Radiat Isot* 70(8):1595–1602.
- Reimer PJ, Brown TA, Reimer RW (2004) Discussion: Reporting and calibration of post-bomb ^{14}C data. *Radiocarbon* 46(3):1299–1304.
- Reimer R, Reimer P (2010) CALIBomb-calibration of post-bomb C-14 data. <http://calib.qub.ac.uk/>.
- Levin I, Hammer S, Kromer B, Meinhardt F (2008) Radiocarbon observations in atmospheric CO_2 : Determining fossil fuel CO_2 over Europe using Jungfraujoch observations as background. *Sci Total Environ* 391(2–3):211–216.
- Cords M (1986) Interspecific and intraspecific variation in diet of two forest guenons, *Cercopithecus ascianus* and *C. mitis*. *J Anim Ecol* 55:811–827.
- Lee PC, Sayialel S, Lindsay WK, Moss CJ (2012) African elephant age determination from teeth: Validation from known individuals. *Afr J Ecol* 50:9–20.
- Laws R (1966) Age criteria for the African elephant, *Loxodonta africana*. *East African Wildlife Journal* 4:1–37.
- Fisher DC (2008) Taphonomy and paleobiology of the Hyde Park mastodon. *Palaeontographica Americana* 61:197–289.
- Fisher D, Beld S, Rountrey A, Allmon W, Nester P (2008) Tusk record of the North Java mastodon. *Palaeontographica Americana* 61:417–463.
- Passey BH, et al. (2005) Inverse methods for estimating primary input signals from time-averaged isotope profiles. *Geochim Cosmochim Acta* 69(16):4101–4116.
- Dirks W, Bromage TG, Agenbroad LD (2012) The duration and rate of molar plate formation in *Palaeoloxodon cypristes* and *Mammuthus columbi* from dental histology. *Quat Int* 255:79–85.
- Metcalfe JZ, Longstaffe FJ (2012) Mammoth tooth enamel growth rates inferred from stable isotope analysis and histology. *Quat Res* 77:424–432.
- Metcalfe JZ, Longstaffe FJ, Ballenger JAM, Haynes CV, Jr. (2011) Isotopic paleoecology of Clovis mammoths from Arizona. *Proc Natl Acad Sci USA* 108(44):17916–17920.
- Wittemyer G, Cerling TE, Douglas-Hamilton I (2009) Establishing chronologies from isotopic profiles in serially collected animal tissues: An example using tail hairs from African elephants. *Chem Geol* 267(1–2):3–11.
- Fricke HC, O'Neil JR (1996) Inter- and intra-tooth variation in the oxygen isotope composition of mammalian tooth enamel phosphate: Implications for palaeoclimatological and palaeobiological research. *Palaeogeogr Palaeoclimatol Palaeoecol* 126(1):91–99.
- Passey BH, Cerling TE (2002) Tooth enamel mineralization in ungulates; implications for recovering a primary isotopic time-series. *Geochim Cosmochim Acta* 66(18):3225–3234.
- Higgins P, MacFadden BJ (2009) Seasonal and geographic climate variabilities during the Last Glacial Maximum in North America: Applying isotopic analysis and macro-physical climate models. *Palaeogeogr Palaeoclimatol Palaeoecol* 283(1):15–27.
- Hynek SA, et al. (2012) Small mammal carbon isotope ecology across the Miocene–Pliocene boundary, northwestern Argentina. *Earth Planet Sci Lett* 321:177–188.
- Koch P, Fisher D, Dettman D (1989) Oxygen isotope variation in the tusks of extinct proboscideans: A measure of season of death and seasonality. *Geology* 17(6):515.
- Hoppe KA, Stover SM, Pascoe JR, Amundson R (2004) Tooth enamel biomineralization in extant horses: Implications for isotopic microsampling. *Palaeogeogr Palaeoclimatol Palaeoecol* 206(3):355–365.
- Kohn MJ (2004) Comment: Tooth enamel mineralization in ungulates: Implications for recovering a primary isotopic time-series, by BH Passey and TE Cerling (2002). *Geochim Cosmochim Acta* 68(2):403–406.
- Codron J, et al. (2012) Stable isotope series from elephant ivory reveal lifetime histories of a true dietary generalist. *Proc Biol Sci* 279(1737):2433–2441.
- Rountrey AN, Fisher DC, Vartanyan S, Fox DL (2007) Carbon and nitrogen isotope analyses of a juvenile woolly mammoth tusk: Evidence of weaning. *Quat Int* 169:166–173.
- Dean MC, Scandrett AE (1996) The relation between long-period incremental markings in dentine and daily cross-striations in enamel in human teeth. *Arch Oral Biol* 41(3):233–241.
- Reid DJ, Dean MC (2006) Variation in modern human enamel formation times. *J Hum Evol* 50(3):329–346.
- Fisher DC (1987) Mastodon procurement by paleoindians of the Great Lakes Region: Hunting or scavenging? *The Evolution of Human Hunting*, eds Nitecki MH, Nitecki DV (Plenum, New York), pp 309–421.
- Fisher DC (2001) Season of death, growth rates, and life history of North American mammoths. *Proceedings of the International Conference on Mammoth Site Studies*. University of Kansas Publications in Anthropology (Univ of Kansas, Lawrence, KS), Vol 22, pp 121–135.
- Roe D, et al. (2002) *Making a Killing or Making a Living: Wildlife Trade, Trade Controls, and Rural Livelihoods*. Biodiversity and Livelihoods Issues (Int Inst for Environment and Development, London), Vol 4.
- US Department of State (2007) Countering multi-billion dollar illegal wildlife trade focus of government-backed global coalition (Bureau of Oceans and International Environmental and Scientific Affairs, Washington, DC).
- Wasser S, et al. (2010) Conservation. Elephants, ivory, and trade. *Science* 327(5971):1331–1332.
- Convention on International Trade in Endangered Species of Wild Fauna and Flora (2010) Monitoring of illegal hunting in elephant range states (CITES, Châtelineau, Geneva), CoP15, Doc. 44.2 (Rev. 1).
- Wittemyer G, Daballen D, Douglas-Hamilton I (2013) Comparative demography of an at-risk African elephant population. *PLoS ONE* 8(1):e53726.
- Wasser SK, et al. (2004) Assigning African elephant DNA to geographic region of origin: Applications to the ivory trade. *Proc Natl Acad Sci USA* 101(41):14847–14852.
- Vogel J, Eglinton B, Auret J (1990) Isotope fingerprints in elephant bone and ivory. *Nature* 346(6286):747–749.
- Van der Merwe N, et al. (1990) Source-area determination of elephant ivory by isotopic analysis. *Nature* 346(6286):744–746.
- Trapani J, Fisher DC (2003) Discriminating proboscidean taxa using features of the Schreger pattern in tusk dentin. *J Archaeol Sci* 30(4):429–438.